

We really appreciate your thoughtful and constructive comments, which were all considered for the revision. The ambiguity that referees pointed out mainly arises from omission or soothing due to a large set of data including long-term, intensive, and vertical measurements at different sites. They were all clarified, and the manuscript was heavily modified. The responses are given with the parts of revised manuscript.

Anonymous Referee #2

<General comments>

This paper discusses the formation mechanism of aerosols in northeast Asia. The authors used in-situ data obtained in Jeju Island from January 2013 to December 2016 and those during KORUS-AQ (May-June 2016) to investigate the variability in aerosol concentrations in the boundary layer. They used the empirical orthogonal function (EOF) analysis to classify the observed features. While the main topic of this paper is suitable for ACP, I do not think that the main conclusions are fully supported by observational evidence. I suggest that the authors largely reorganize the results and discussion and clarify the robust and new findings from this study. I recommend major revisions.

<Specific comments>

Introduction

The formation of aerosols associated with meteorological cycles (e.g., anticyclones, cyclones, and air stagnation) has been extensively studied either in continental source areas or downwind regions. Variability in vertical profiles of aerosols associated with the evolution of the boundary layer has also been extensively investigated. Although this study might be the first to present such data in Korea, I think the fundamental mechanisms are common in many cases. The authors should briefly review previous studies in northeast Asia (e.g., TRACE-P, CARE-Beijing) and also in other regions, and discuss the similarity and difference between this study and previous ones. Here are some examples of the previous studies in northeast Asia.

Weber, R. J., et al. (2003): J. Geophys. Res., 108, 8814, doi:10.1029/2002JD003112.

Matsui, H., et al. (2009): J. Geophys. Res., 114, D00G13, doi:10.1029/2008JD010906.

Takegawa, N., et al. (2009): J. Geophys. Res., 114, D00G05, doi:10.1029/2008JD010857.

Haenel, A., et al. (2012): J. Geophys. Res., 117, D13201, doi:10.1029/2012JD017577.

Wang, J., et al., (2019): Atmos. Chem. Phys., 19, 8845-8861, doi:10.5194/acp-19-8845-2019.

The following review paper would also be useful for the interpretation of NPF events in relation with meteorological conditions.

Kerminen, V.-M., et al. (2018), *Environ. Res. Lett.*, 13, 103003. doi:10.1088/1748-9326/aadf3c.

Thank you for references. They were referred in the revised manuscript as follows.

L84:

(Kerminen et al., 2018).

L89:

Nucleation-mode particles were often observed under the clean background conditions (Song et al., 2010; Weber et al., 2003).

L98-115:

Recently, meteorological conditions are thought to be closely related to persistent PM_{2.5} haze pollution over China on a regional scale (Wang et al., 2014c, 2014b, 2019; Zhang et al., 2018). Strong correlations of daily PM_{2.5} concentrations with several meteorological variables (local or climate variables) have been found and unambiguous spatial patterns indicate the importance of synoptic meteorology affecting haze developments (Cai et al., 2017; Leung et al., 2018). Among these, the dynamic evolution of planetary boundary layer (PBL) has drawn much attention due to its direct effects on PM_{2.5} concentrations such as stable atmospheric stratification accumulating local emissions, positive feedback between boundary layer stability and pollution intensity, and downward transport of pollutants from the free atmosphere through PBL processes (Li et al., 2020; Quan et al., 2020; Zhong et al., 2018). In addition, entrainment through the boundary layer has been suggested as an important mechanism for enhancing surface O₃ (Hu et al., 2018; Lee et al., 2003). For NPF, the combined effect of boundary layer dynamics and atmospheric chemistry on aerosol composition was emphasized (Hao et al., 2018; Song et al., 2010). As is commonly observed during several haze events, high relative humidity (RH) is believed to facilitate the hygroscopic growth of secondary inorganic aerosols, thereby increasing PM_{2.5} concentrations (Wang et al., 2019; Zhang et al., 2015). However, a comprehensive and systematic understanding of particle formation/transformation and haze developments is hindered by the complexity of local to large-scale meteorology, local emissions versus transboundary transport of pollutants, and particle (trans)formation mechanisms. Therefore, long-term observations in the background region are essential to better understand the phenomena on a regional scale.

L144-146: Uncertainty in the coating thickness

The estimation of coating thickness of BC particles from SP2 data, although it has been used by many investigators, may contain significant uncertainties. The authors selected a BC core

diameter of 200 +/- 20 nm. Why did the authors select this specific diameter? Is it reasonable to estimate a coating thickness of > 10 nm with the core diameter uncertainty of 20 nm?

Detailed information was added to the text as follows.

L181-187:

The coating thickness of individual rBC particles was determined as $(D_{\text{shell}} - D_{\text{rBC}})/2$. In this SP2, D_{shell} was detectable in the range of 170 nm ~ 500 nm. The proper range of D_{rBC} for LEO approach varies mainly depending on the instrumental setup of the SP2. To ensure the quality of LEO results, lower and upper bounds of D_{rBC} are selected by examining detectable optical diameter of small rBC core (here, $\geq 95\%$) and a saturation point of the low gain scattering detector (Taylor et al., 2015). In the present study, D_{rBC} for LEO approach was restricted to the rBC core with a D_{rBC} of 180-220 nm (Laborde et al., 2012b, 2013; Zanatta et al., 2018).

L249-251: Boundary layer stability

The dominance of a high-pressure system (subsidence) generally leads to the formation of strong inversions and stable boundary layers. The description in this paragraph seems to be opposite.

Weather conditions of the two modes were described in detail in Sect. 3.3, where averaged characteristics and daily evolution of meteorological variables and aerosol properties are shown in Figure 3 and Figure 4.

In general, the more incoming solar radiation heats the surface and induces the deep vertical mixing under clear sky while high pressure system resides over the study region.

L259-269: Entrainment

The authors conclude that the rapid increase in PM_{2.5} was due to the entrainment of particles from upstream areas. The authors state that elevation of aerosol concentrations is “believed” to occur by the intrusion of pollutants from the upper atmosphere. What is the basis for this statement? I do not think that the descriptions in this paragraph are supported by observational evidence.

It is not PM_{2.5} but nano particles that were entrained into the boundary layer. The vertical profiles of particle_{3.5 nm-0.3 μm}, particle_{0.3-0.5 μm}, and particle_{0.5-1.0 μm} are compared between the “persistent anticyclone” and “transport/haze” periods (Figure 6), which were obtained from balloon measurement during the KORUS-AQ study. The relevant parts are given below. Later, results of previous studies were introduced, which were in agreement with our observation.

L362-374 :

The high surface temperature resulted in a deep mixing layer on May 20 of “persistent anticyclone” period (Fig. 6a). The particle number concentrations at all size ranges were low over the altitude, explained by dilution of pre-existing particles by vertical mixing. In contrast, in the morning on May 25 (“transport/haze” period), the mixed layer was shallow with a temperature inversion layer at about 1000 m (top gray box in Fig. 6b). The morning profile illustrates visibly high concentrations of the particle_{3.5 nm-0.3 μm} (about 10^4 cm^{-3}) both at surface and at around the inversion (gray boxes in Fig. 6b). The high concentration near the surface is attributed to fresh emissions in the morning. On the other hand, high number of particle_{3.5 nm-0.3 μm} at around the inversion is similar to the results of previous studies in which a large number of ultrafine particles were commonly found above the cloud as a result of an enhanced photochemical reaction (Clarke, 1993). In the afternoon, the thin layer laden with large amount of particle_{3.5 nm-0.3 μm} disappeared, but the number of accumulation mode particles (particle_{0.3-0.5 μm} and particle_{0.5-1.0 μm}) increased remarkably, particularly at altitudes between 1000~1500 m (Fig. 6c). It is evident for the evolution of nucleation- and Aitken-mode particles existing in the inversion layer, as the PBL developed.

L382-387:

Recently, it was suggested that pollutants were carried from the upstream areas in the upper layer by westerly winds, remained above the nocturnal boundary layer, and entrained into the PBL during the day; this led to a high PM₁₀ concentration at the surface of Seoul (Lee et al., 2019). The PM_{2.5} haze pollution was accompanied with a strong temperature inversion in downwind regions of polluted northeast China (Shi et al., 2020). Therefore, these results indicate that the rapid increase in PM_{2.5} mass in Northeast Asia could be closely coupled with the development of the PBL.

L306-318: Gas-to-particle conversion.

The discussion in this paragraph is highly speculative. The partitioning between HNO₃ and NH₄NO₃ should be explicitly investigated to discuss the gas-to-particle conversion for nitrate aerosols. See, for example, Neuman, J. A., et al. (2003): J. Geophys. Res., 108, 4557, doi:10.1029/2003JD003616. Furthermore, the formation of (NH₄)₂SO₄ might be controlled by

aqueous-phase reactions in cloud droplets rather than condensation processes. Please reconsider the interpretation.

This part was modified as follows.

L400-403:

It is likely that the mixing through inversion layer caused hygroscopic growth of existing nucleation- and Aitken-mode particles, which led to an increase in the number of accumulation-mode particles where the water-soluble vapors readily condensed, adding mass to the particles.

L353-366: Interpretation of the coating thickness

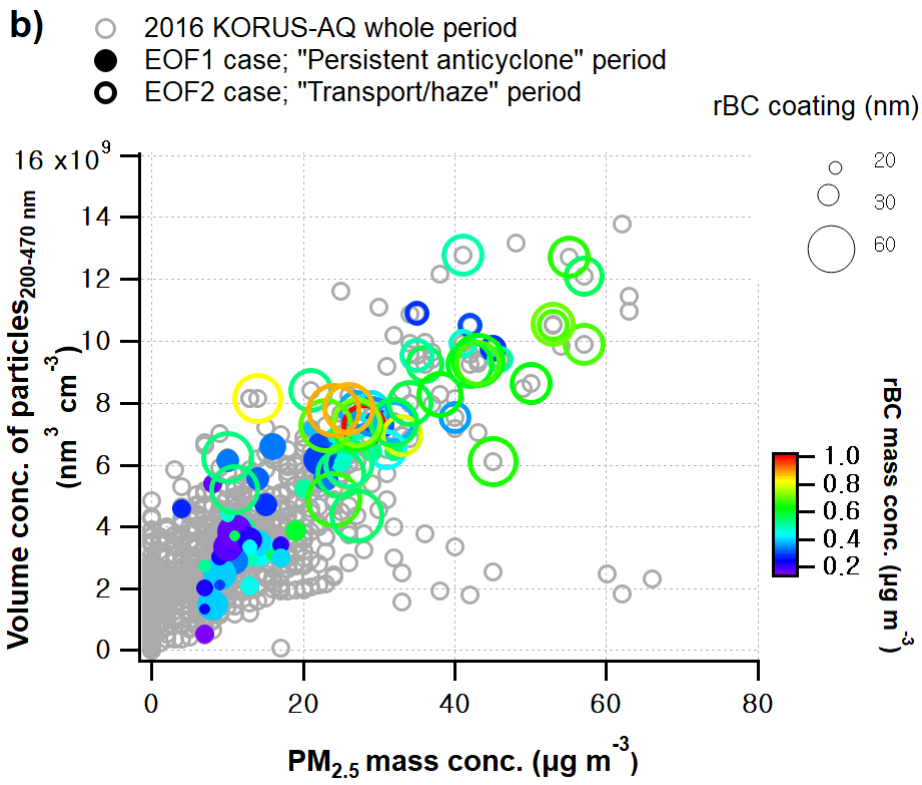
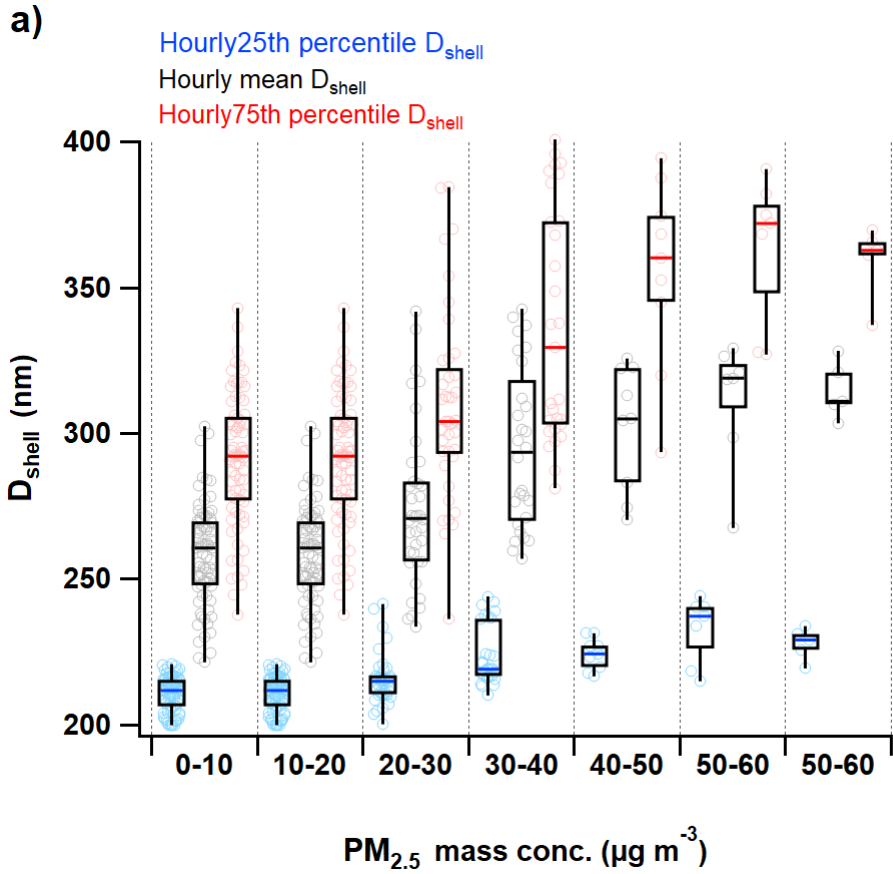
The authors suggest that the coating thickness of rBC is a useful parameter to understand the formation of secondary aerosols, and also suggest that reducing BC emissions is the effective way to reduce PM_{2.5} in Asia. I think the descriptions in these paragraphs are also very speculative and not supported by observational evidence. Fig. 7 seems to be the basis for this hypothesis, but I find many data points at lower aerosol mass loadings with thick coatings. It may be true that the EOF2 case can be characterized by high PM_{2.5} and thick coatings, but it does not necessarily mean that the coating thickness is the controlling factor. I would guess the correlation between the PM_{2.5} concentrations and the coating thickness is rather weak. Please show more convincing data to support the hypothesis. Otherwise I recommend that the authors should remove (at least tone down) this conclusion.

This part was rephrased and Figure 7a was added.

L423-445:

Figure 7a illustrates variations of D_{shell} (optical diameter of rBC-containing particle in a core-shell configuration with rBC core-restricted to 180-220 nm; Sec. 2.1) as a function of PM_{2.5} concentration bin for the entire campaign period. D_{shell} increased almost linearly with PM_{2.5} mass concentration, reaching 300-400 nm on average at PM_{2.5} higher than 40 $\mu\text{g m}^{-3}$. This reveals a close relationship between rBC coating thickness and PM_{2.5} mass enhancements. In Figure 7b, volume concentration of particles_{200-470 nm} was also elevated simultaneously with PM_{2.5} mass concentrations, and rBC coating was obviously thicker (48 ± 39 nm) during "transport/haze" period when the PM_{2.5} mass concentration was highly elevated over the Korean peninsula (Jordan et al., 2020). These results demonstrate that rBC-containing particles with thick coatings are truly representative of accumulation-mode particles in terms of size particularly during "transport/haze" period. Together with the enhanced SIA

concentrations and the thicker coating of rBC (Fig. 7b and c), ALWC was as high as $10.3 \pm 8.2 \mu\text{g m}^{-3}$, accounting for 30% of the dry $\text{PM}_{2.5}$ mass (Fig. 7c and Table 2). Given that the RH remained high at greater than 60% during the day and up to 90% at night (Fig. 7b), hygroscopic growth of NH_4NO_3 and $(\text{NH}_4)_2\text{SO}_4$ by uptake of water was expected to be promoted, leading to a large increase in ALWC. SOR was almost linearly increased with RH (Fig. S8b and d). More importantly, sulfuric acid is known to readily condenses on the rBC surface (Kiselev et al., 2010; Zhang et al., 1993, 2008), which provides an active surface for heterogeneous reaction by changing its hygroscopic properties (Khalizov et al., 2009). Hence, the characteristic features observed during the “transport/haze” period suggest an effective condensation of vapors to rBC surfaces and reaction with SIA, resulting subsequent growth of rBC particles in size and mass by forming thick coating on their surfaces (Adachi et al., 2014; Lim et al., 2018; Ueda et al., 2016). The shell size of rBC with a core diameter of 180-220 nm reached approximately 300-400 nm. Given that the $\text{PM}_{2.5}$ concentration increased linearly with the volume concentration of particles_{200-470 nm} (Fig. 7a), the role of internally-mixed BC particles is critical to the increase in mass of fine aerosol, as they provide surfaces for gaseous precursors of SIA to condense on.



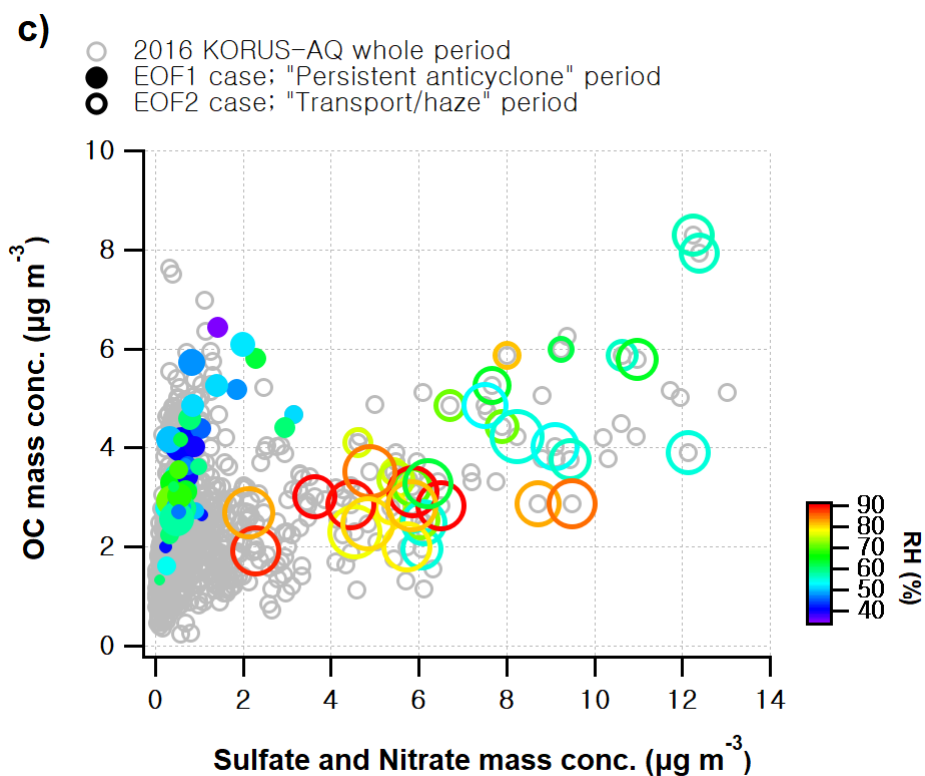


Figure 7.

<Minor comments>

L73-74, L182: SO₂, NO_x, and VOCs are not "condensable" gases but precursors.

They were all changed throughout the manuscript.

L100-121: Please specify the model number of the SMPS, CPC, and OPC. Please also describe how these instruments were evaluated and calibrated. It is not necessary to capitalize the first character of the name of the instruments.

L130:

the scanning mobility particle sizer (SMPS, model 3034, TSI, USA).

L146-152:

Aerosol number concentrations were measured by lab-made instruments at Hanyang University including condensation particle counter (CPC) for particles larger than 3 nm and two

optical particle counters (OPC) for accumulation-mode particles (particle_{0.3-0.5 μm} and particle_{0.5-1.0 μm}) (Lee et al., 2014). The number concentration of nanoparticles (particle_{0.3 nm-0.5 μm}) was reported as difference between CPC and OPC. For CPC and OPCs, sampling rate and counting resolution was 0.125 L min⁻¹ and 1 s, respectively. The results of vertical measurements using these instruments can be found elsewhere (Querol et al., 2017, 2018).

L178-179: I do not think the estimate of GR values has three significant digits.

They were all corrected as follows.

L223: GR₁₀₋₅₀ of $2.1 \pm 1.6 \text{ nm h}^{-1}$

L227: CS_{100-470nm} equal to 1.3 ± 0.9

L234: CS_{100-470nm} (1.8 ± 1.0)

Table 1 : GR and CS

L331: "peaking below 100 nm" - Please specify number, surface, or mass.

L417:

Peaking below 100 nm in number

General Comments:

This manuscript describes in situ observations of aerosol size distributions and composition at a rural site on the Korean peninsula, with occasional vertical aerosol concentration information provided by nearby instrumented balloon launches. The work highlights two characteristic daily patterns of aerosol size distributions, a new particle formation EOF and a haze or accumulation-mode dominated EOF. A key question raised by the authors is what drives the development of high PM_{2.5} loading in this region, and the size distributions observations are compared with meteorological conditions as well as physico-chemical observations of black carbon aerosol.

My main comment is that the argument that meteorological differences define the two EOF features is not well-supported by the analysis presented in the paper. In fact, the meteorological description of the periods is not consistent with the description provided on the same measurement period in this work, which is cited once in the present work:

Peterson, DA, et al. 2019. Meteorology influencing springtime air quality, pollution transport, and visibility in Korea. *Elem Sci Anth*, 7: 57. DOI: <https://doi.org/10.1525/elementa.395>

Peterson et al. characterize the period of May 17-22 as "stagnation under a persistent anticyclone" and the period May 25-21 as "dynamic meteorology, low-level transport, and haze development", whereas in the present work (to the best of my understanding) that earlier period is described as "persistent anticyclone" (associated with EOF1) and the 2nd period as "synoptic-scale stagnation" (associated with EOF2). There seems to be a disconnect here. The caption of Figure 6 is consistent with the Peterson paper, but the abstract and perhaps the rest of the present manuscript are not. Furthermore, to my (perhaps untrained) eye, the meteorological patterns plotted in Fig 4a. and 4b. do not appear to be very different. Both appear to be fairly dynamic, quite distinct from the stagnant/blocking pattern shown in Fig. 4c. of Peterson et al.

A related issue is that the terms EOF1 and EOF2 are used fairly loosely in the manuscript. I understand them to be defined by a statistical treatment of the size distribution data and refer to two specific patterns of aerosol size development over a day. But these terms are used to represent actual time periods as well, e.g. in Figure 4 where the geopotential height averaged over EOF1 and EOF2 is given. What time periods are actually represented there? Are they EOF1 and 2 periods over the multi-year data set or during the KORUS-AQ measurement period? I advise the authors to use different terms to define time periods in the multi-year data set and the KORUS measurement period.

For 4-year measurement data, the days having the highest 10 % scores of EOF1 and EOF2 were extracted, and their physical and chemical properties were compared in the manuscript. The EOF analysis used in this study was described in more detail as follows.

L204-206:

Continuous measurements of size-separated number concentrations, spanning four years from 2013 to 2016, were analyzed using an empirical orthogonal function (EOF) method, in which the loading vector was constrained to be periodic with a 24-hour period (e.g., Kim et al., 2014).

During the KORUS-AQ campaign, 4 distinct episodes were distinguished, among which “persistent anticyclone” and “transport/haze development” correspond to EOF 1 and EOF 2, respectively. The campaign was conducted during May~June. Figure 4 shows geopotential height and trajectories averaged for the top 10 % EOF1 and EOF2 days for 4 years. Therefore, the detailed features were averaged out. This figure was moved to supplementary information (Figure S4). Please see Figure 3 in the revised manuscript, presenting the monthly characteristics of EOF and EOF2.

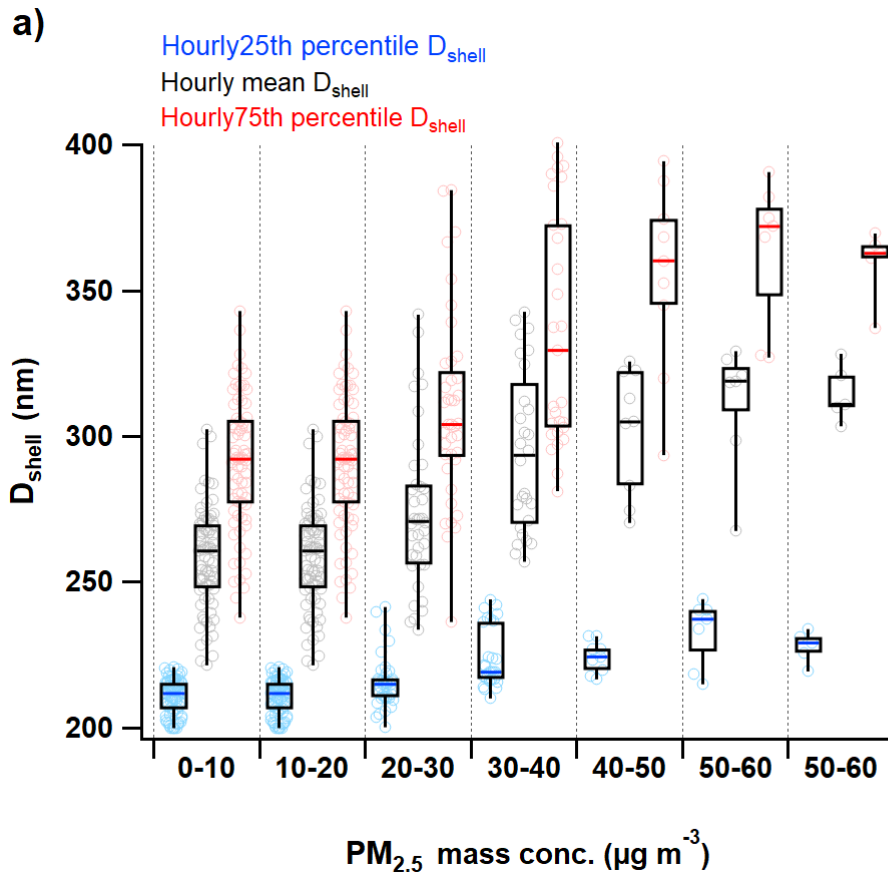
I found the discussion of black carbon coating thickness as a useful diagnostic tool for the prevalent aerosol formation processes to be a very interesting concept and well-supported by the observations presented.

This part was refined with Figure 7a as follows.

L423-445:

Figure 7a illustrates variations of D_{shell} (optical diameter of rBC-containing particle in a core-shell configuration with rBC core-restricted to 180-220 nm; Sec. 2.1) as a function of $\text{PM}_{2.5}$ concentration bin for the entire campaign period. D_{shell} increased almost linearly with $\text{PM}_{2.5}$ mass concentration, reaching 300-400 nm on average at $\text{PM}_{2.5}$ higher than $40 \mu\text{g m}^{-3}$. This reveals a close relationship between rBC coating thickness and $\text{PM}_{2.5}$ mass enhancements. In Figure 7b, volume concentration of particles_{200-470 nm} was also elevated simultaneously with $\text{PM}_{2.5}$ mass concentrations, and rBC coating was obviously thicker (48 ± 39 nm) during “transport/haze” period when the $\text{PM}_{2.5}$ mass concentration was highly elevated over the Korean peninsula (Jordan et al., 2020). These results demonstrate that rBC-containing particles with thick coatings are truly representative of accumulation-mode particles in terms of size particularly during “transport/haze” period. Together with the enhanced SIA concentrations and the thicker coating of rBC (Fig. 7b and c), ALWC was as high as $10.3 \pm 8.2 \mu\text{g m}^{-3}$, accounting for 30% of the dry $\text{PM}_{2.5}$ mass (Fig. 7c and Table 2). Given that the RH remained high at greater than 60% during the day and up to 90% at night (Fig. 7b), hygroscopic growth of NH_4NO_3 and $(\text{NH}_4)_2\text{SO}_4$ by uptake of water was expected to be promoted, leading to a large increase in ALWC. SOR was almost linearly increased with RH (Fig. S8b and d). More importantly, sulfuric acid is known to readily condense on the rBC surface (Kiselev et al., 2010; Zhang et al., 1993, 2008), which provides an active surface for heterogeneous reaction by changing its hygroscopic properties (Khalizov et al., 2009). Hence, the

characteristic features observed during the “transport/haze” period suggest an effective condensation of vapors to rBC surfaces and reaction with SIA, resulting subsequent growth of rBC particles in size and mass by forming thick coating on their surfaces (Adachi et al., 2014; Lim et al., 2018; Ueda et al., 2016). The shell size of rBC with a core diameter of 180-220 nm reached approximately 300-400 nm. Given that the $PM_{2.5}$ concentration increased linearly with the volume concentration of particles_{200-470 nm} (Fig. 7a), the role of internally-mixed BC particles is critical to the increase in mass of fine aerosol, as they provide surfaces for gaseous precursors of SIA to condense on.



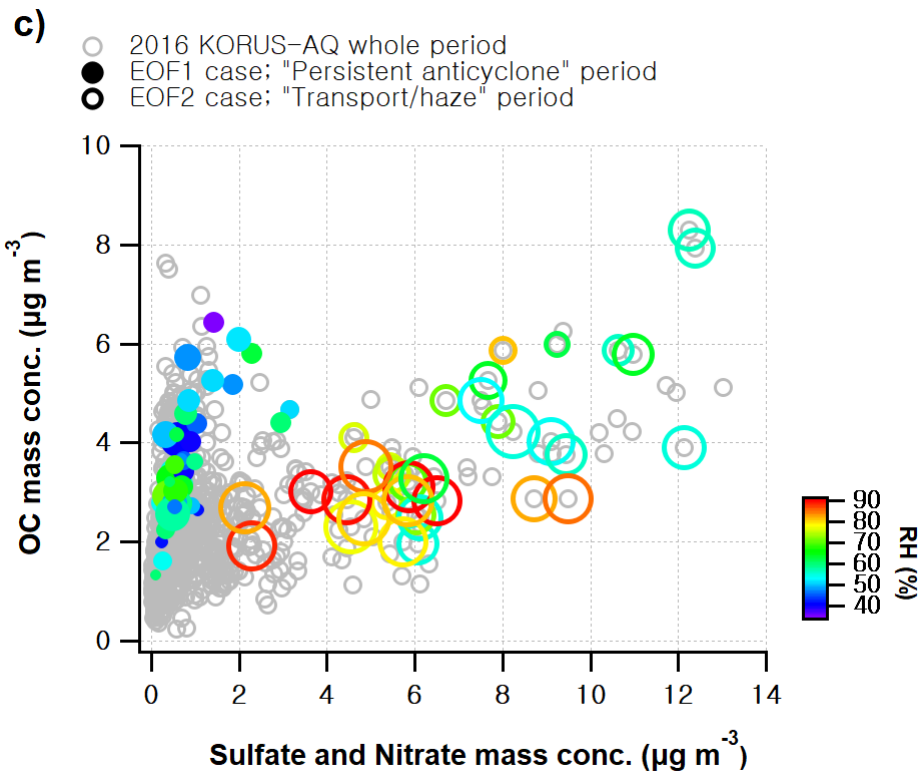
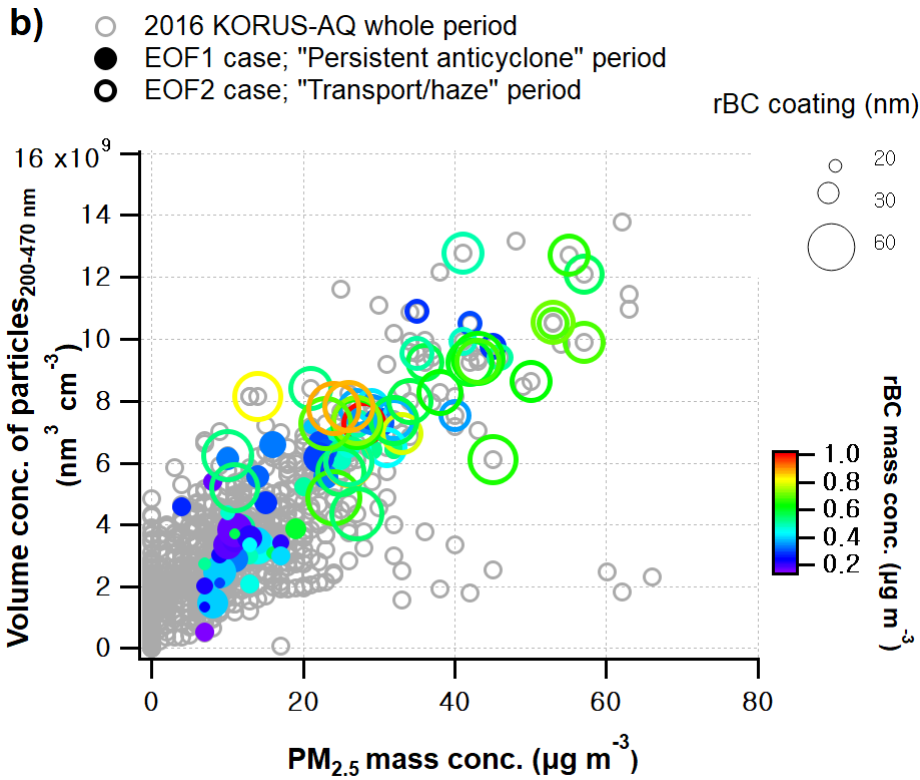


Figure 7. Relationships of rBC properties, PM_{2.5} mass and composition, and particles₂₀₀₋₄₇₀ volume concentration measured during the KORUS-AQ campaign. (a) D_{shell} variations

as a function of $PM_{2.5}$ concentration for the whole campaign period, (b) relationship between particles₂₀₀₋₄₇₀ volume concentration and $PM_{2.5}$ mass concentration color-coded by rBC mass concentration, and (c) relationship between $PM_{2.5}$ chemical constituents color-coded by RH. In (b) and (c), the marker size is proportional to the rBC coating thickness. D_{shell} and coating thickness are restricted to $180 \text{ nm} \leq D_{rBC} \leq 220 \text{ nm}$.

L175-187:

Basically, adopting the leading-edge-only approach (LEO approach; Gao et al., 2007; Laborde et al., 2012a), the optical diameter of the rBC-containing particle, D_{shell} , was inferred from the leading-edge scattering signal using Mie theory with Refractive Index (RI) of $1.5 - 0i$ and $2.26 - 1.26i$ for the rBC coating material and rBC core, respectively, at an SP2 operating wavelength of 1064 nm. These RI values have been suggested in previous studies: $2.26 - 1.26i$ for bare or freshly-emitted ambient rBC particles (Moteki and Kondo, 2010; Taylor et al., 2015) and $1.5 - 0i$ for inorganic salts and secondary organic aerosol (Schnaiter et al., 2003; Toon et al., 1976) have been used for similar LEO approaches (e.g., Laborde et al., 2013; Schwarz et al., 2008). The coating thickness of individual rBC particles was determined as $(D_{shell} - D_{rBC})/2$. In this SP2, D_{shell} was detectable in the range of 170 nm ~ 500 nm. The proper range of D_{rBC} for LEO approach varies mainly depending on the instrumental setup of the SP2. To ensure the quality of LEO results, lower and upper bounds of D_{rBC} are selected by examining detectable optical diameter of small rBC core (here, $\geq 95\%$) and a saturation point of the low gain scattering detector (Taylor et al., 2015). In the present study, D_{rBC} for LEO approach was restricted to the rBC core with a D_{rBC} of 180-220 nm (Laborde et al., 2012b, 2013; Zanatta et al., 2018).

L465-469:

In this regard, rBC particles and their coating thickness are proposed as an agent for generating accumulation-mode particles through SIA formation and as an operational parameter to understand the chemical mechanisms responsible for fine aerosol pollution driven by SIA, respectably. This, in turn, implies that reducing primary emissions of gaseous precursors and BC will be one of the effective ways to combat high $PM_{2.5}$ mass concentrations in Northeast Asia, especially during the cold months.

My bottom line for publishing this work in ACP is that the authors need to either do a lot more work showing the relationship between the characteristic aerosol EOF periods and synoptic

scale meteorology, or they need to significantly de-emphasize claims of a relationship between them in the paper. In any case the time periods described need to be more clearly defined and not always tagged simply as EOF1 or EOF2.

As you recommended, the manuscript was reconstructed and fully revised.

Specific comments:

Separating the figures from the captions makes the figures difficult to review.

It was modified.

line 72 seems to imply all aerosol particles start from nucleation. Suggest rephrasing.

L81-82:

Theoretically, new particle formation (NPF) and particle's subsequent growth occur via the gas-to-particle conversion of gaseous precursors, which include SO₂, NO_x, VOCs, and NH₃.

line 76 suggest change to "the level of pre-existing particles". As it stands, "a level" seems to imply that there's a minimum threshold of CS to achieve NPF, and I suspect that's not what the authors mean.

It is rephrased as follows.

L83:

(ii) a pre-existing particles that act as a condensation sink (CS) (Kerminen et al., 2018).

Line 169 and Figure S4. How were EOF1 and EOF2 periods determined? Is it just chance that 143 days each were found, or was that purposeful? Is there some threshold PCA value that causes a given time period to be included in the EOF1 or 2 bin?

As stated above, we selected the days having the highest 10 % scores of EOF 1 and EOF 2 among 4-year data to highlight the characteristics of two modes.

Line 177 not sure what exactly is meant here. Are there >10⁴/cm³ particles when only considering 20-30 nm particles?

It is specified to ~10–30 nm particles.

L221:

The nucleation- and Aitken-mode particles dominated number concentrations with the maximum number concentration greater than 10^4 cm^{-3} at ~10–30 nm around noon (Fig. 2c).

Line 188. Same comment as line 177.

It is also specified to 100-130 nm particles.

L233:

5000 cm^{-3} at 100–130 nm

Line 193 "It turned out..." This sentence is very broad and isn't immediately supported by the details of what is meant so it seems out of place.

The sentence is rephrased.

L240-244:

The two EOF modes are supposed to represent physically independent phenomena. If EOF1 characterized the pattern of increase in number concentration by nucleation- and Aitken-mode particles, it is clear that EOF2 diagnosed the case where the number concentration of accumulation-mode particles increased noticeably in the absence of such small particles. However, EOF2 was rarely recognized as an episode because it did not exhibit as prominent evolution in particle number as EOF1.

Line 243. What is meant by a mid-low cloud base height?

L139-140:

In addition, a set of cloud fraction (low-and mid-level clouds; 1-10 in fraction) and the base height of cloud were measured with a ceilometer (CL31, Vaisala),

Line 251. Can you elaborate on why you consider EOF2 to correspond to "stagnant" conditions? To me this implies that in EOF1 there may be higher windspeeds, but this was not observed according to Table 1. In general, I find I am not convinced about the clear meteorological differences between the two cases. To my eye, the geopotential height and wind vector plots look fairly similar for the two EOF cases. This issue arises in Table 2 as well, where the boundary layer is just described in words without any analysis.

For clarity, the manuscript was reconstructed (from Sect. 3.3 to Sect. 3.6.) and more detailed information was provided with new Figures (Figure 3-5). Instead, the geopotential height with wind vector plots were sent to supplementary information (Figure S4), which includes the data of all seasons and thus, the distinct weather patterns were averaged out.

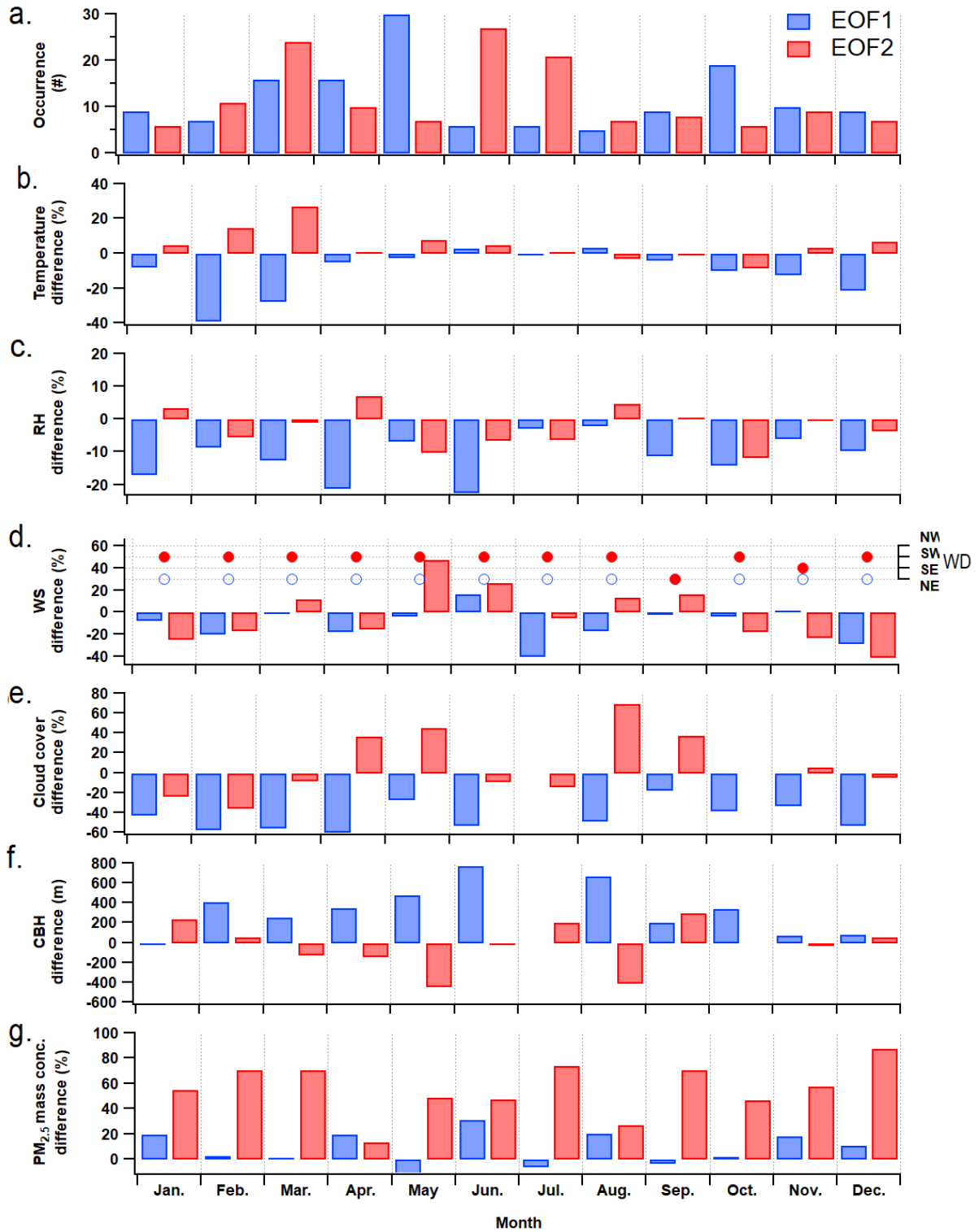
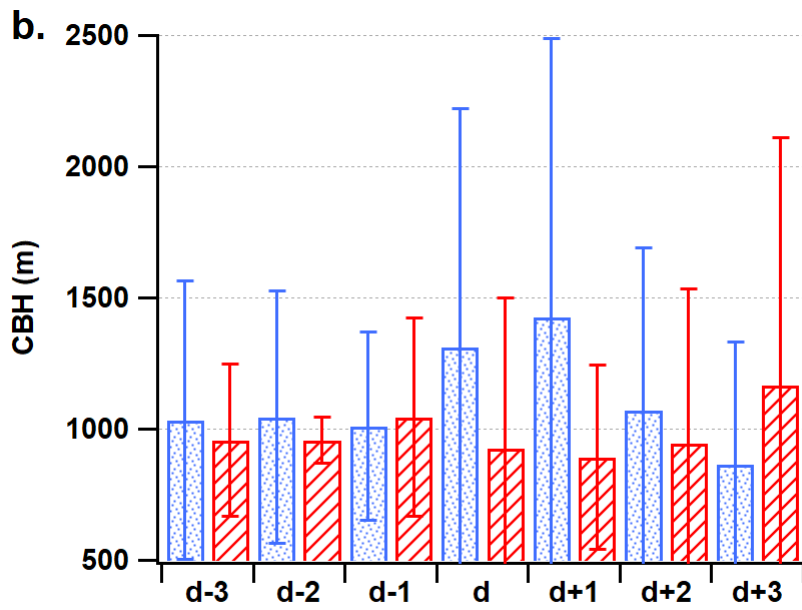
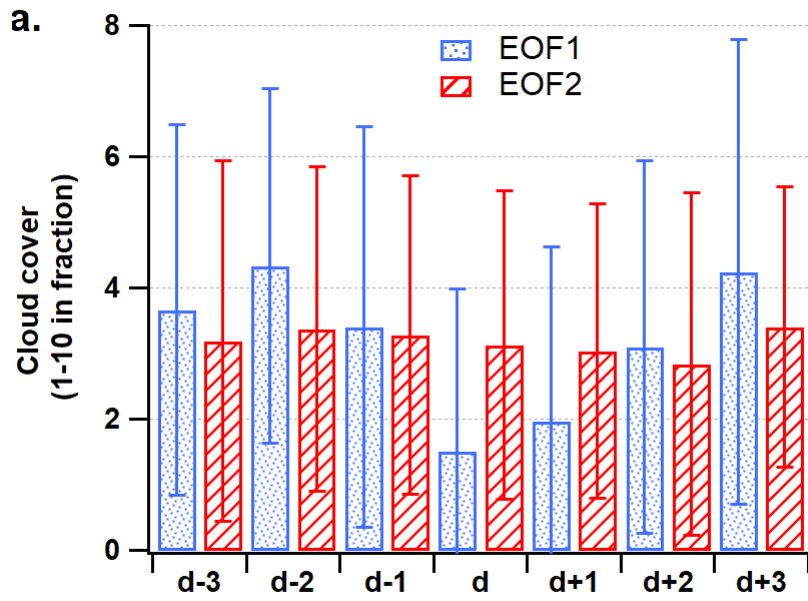
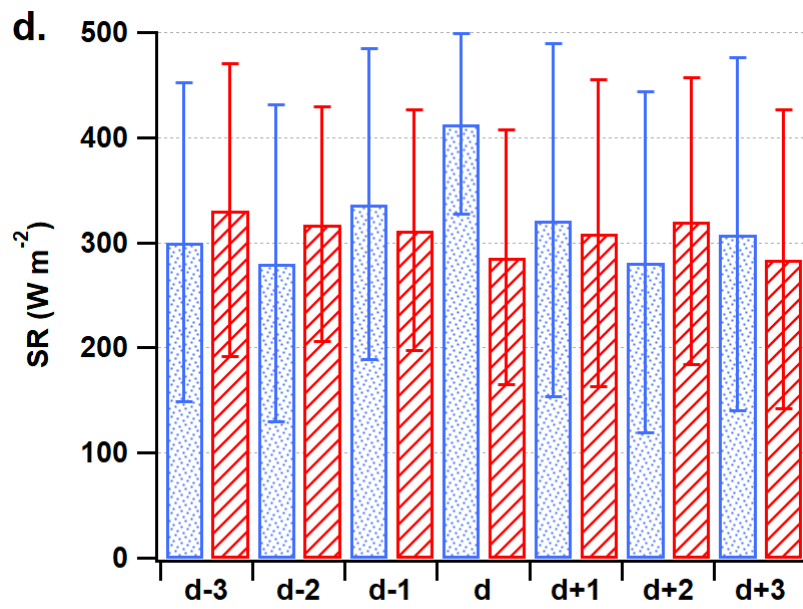
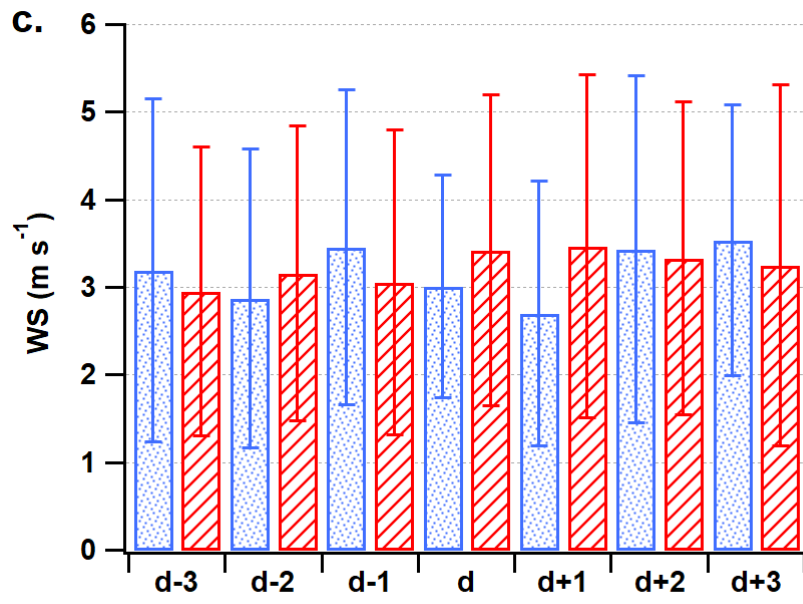


Figure 3. Monthly differences of occurrence, meteorological variables, and PM_{2.5} mass concentration between EOF1 (blue) and EOF2 (red) relative to the monthly means for 2013-2016. (a) Occurrence, (b) Temperature, (c) Relative humidity, (d) Wind speed, (e) Cloud coverage, (f) Cloud base height, and (g) PM_{2.5} mass concentration.





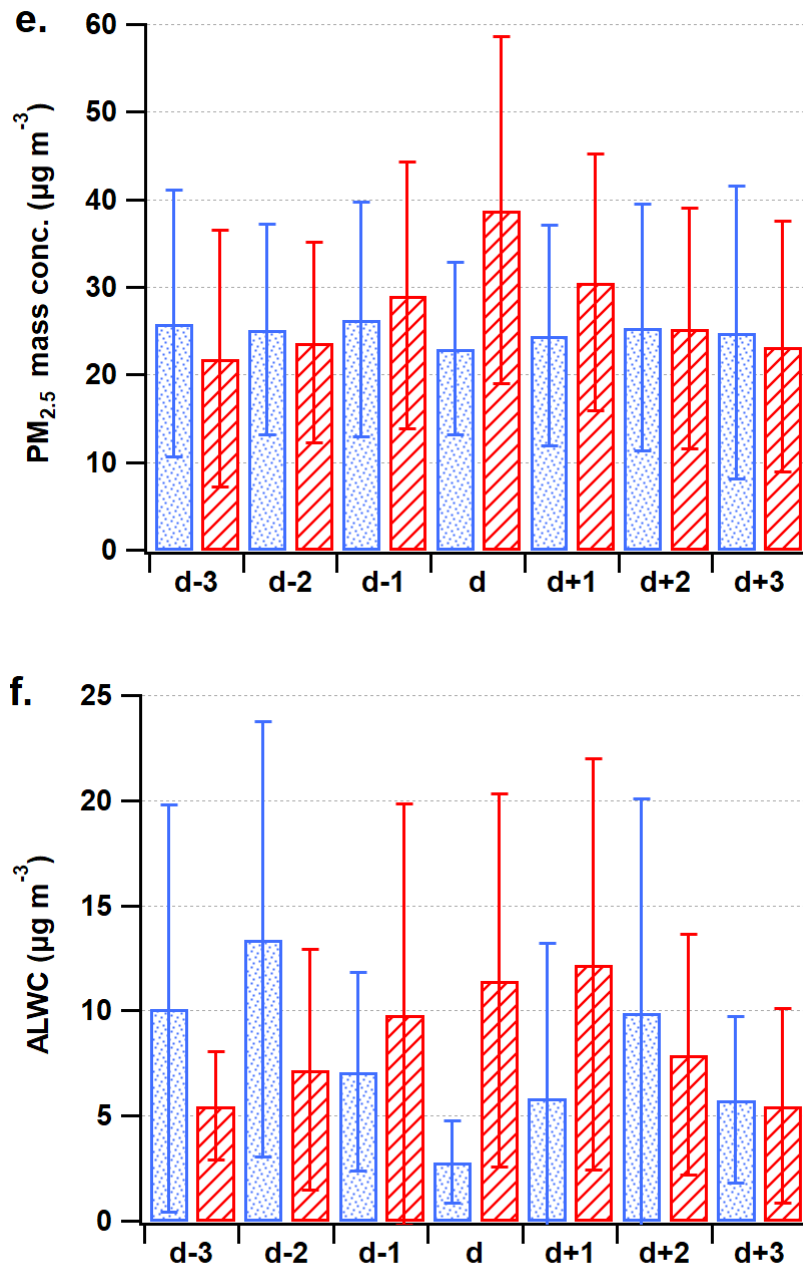


Figure 4. Daily evolutions of meteorological variables, PM_{2.5} mass concentration, and aerosol liquid water content (ALWC) over 7-day course in March of 2013-2016 for EOF1 (blue) and EOF2 (red). The 7-day course includes 3 days before (d-3 ~ d-1) and after (d+1 ~ d+3) EOF day (d) that occurred in March for 4 years. Error bars indicate standard deviations.

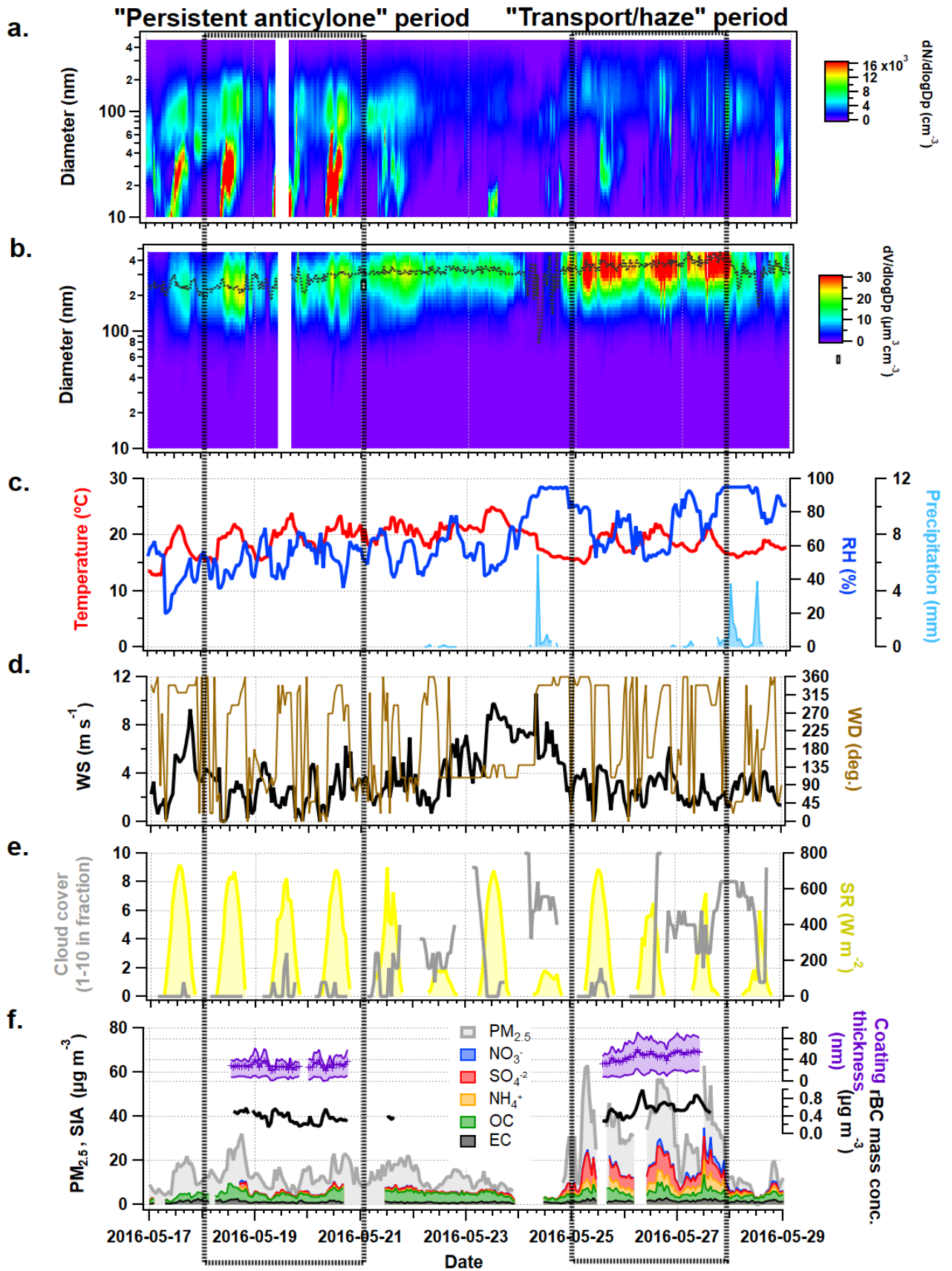


Figure 5. Time-series of aerosol properties and meteorological variables during the 2016 KORUS-AQ campaign. Two periods (May 18-20 and May 25-27) corresponding to EOF1 and EOF2, which are referred to as “persistent anticyclone” and “transport/haze” periods, respectively (indicated by black boxes). (a) Aerosol number size distribution, (b) Aerosol volume size distribution with peak diameter every 30 minutes (black dotted line), (c) Temperature (red), RH (blue), and precipitation (sky blue), (d) WS and Wind direction, (e) Cloud cover and solar radiation (SR), and (f) PM2.5 and SIA mass concentrations and rBC mass concentration (black) and coating thickness (purple; hourly mean, 25th, and 75th percentiles).

Line 308. "burst of particle(>3.5 nm) above 10⁴" needs to be stated more clearly, at least give units for the concentration.

L365-366:

The morning profile illustrates visibly high concentrations of the particle_{3.5 nm-0.3 μm} (about 10⁴ cm⁻²) both at surface and at around the inversion (gray boxes in Fig. 6b).

Line 313-314 "number of >3.5 nm particles tended to be backed up"- not sure what backed up means here.

This sentence was modified as follows.

L397-403:

This layered structure became uniform in the afternoon with the development of the PBL coinciding with elevated RH around the DRH of both (NH₄)₂SO₄ and NH₄NO₃, resulting in a noticeable reduction of particle_{3.5 nm-0.3 μm} and an increase of particle_{0.3-0.5 μm} and particle_{0.5-1.0 μm} in number concentration at altitudes between 1000 m and 1500 m (Fig. 6c). It is likely that the mixing through inversion layer caused hygroscopic growth of existing nucleation- and Aitken-mode particles, which led to an increase in the number of accumulation-mode particles where the water-soluble vapors readily condensed, adding mass to the particles.

Line 306-318. It may be helpful to define a particle size range of >3.5 nm to 0.3 μm. It's a little confusing talking about >3.5 nm particles (which includes the 0.3-0.5 μm and 0.5-1.0 μm particles) as distinct from these other size ranges. I understand most of the number in the >3.5 nm particles must be below 300 nm, but you could make this paragraph significantly clearer by removing >3.5 nm particles and including >3.5-300 nm particles as a size class.

It was modified throughout the manuscript as recommended.

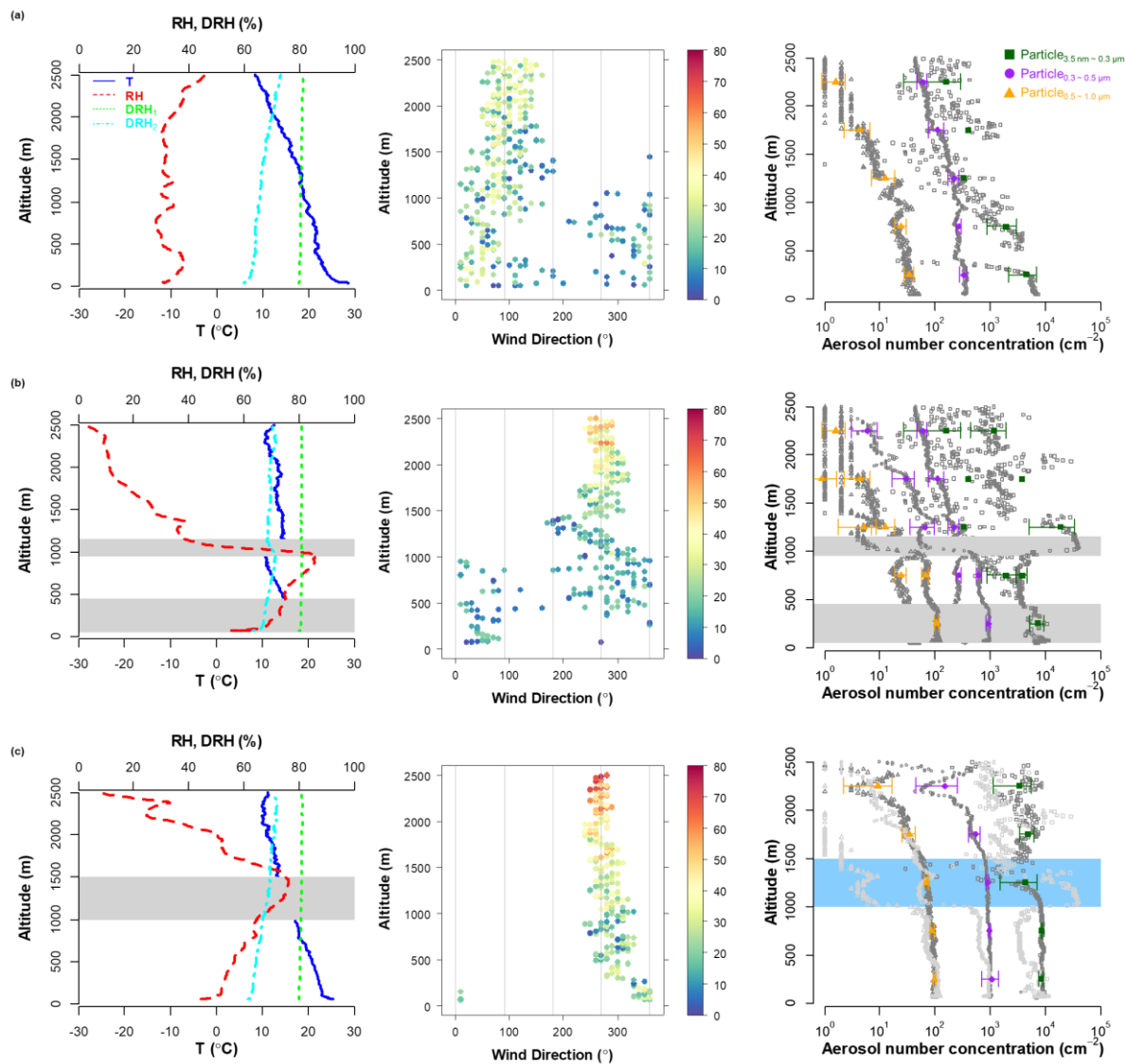


Figure 6. Vertical profiles of meteorological parameters and aerosol number concentrations in SMA during the 2016 KORUS-AQ campaign. (a) Morning time of May 20 during “persistent anticyclone” period, (b) morning time of May 25, and (c) afternoon time of May 25 during “low-level transport and haze development” period. The left panels present ambient temperature (solid blue), RH (dotted red), and deliquescence RH of NH_4NO_3 (sky blue) and $(\text{NH}_4)_2\text{SO}_4$ (green). The middle panels present WD color-coded by WS (km h^{-1}). The right panels present number concentrations (cm^{-2}) of particles with D_p between 3.5 nm and 0.3 μm (particle_{3.5 nm-0.3 μm}) in green, D_p of 0.3–0.5 μm (particle_{0.3-0.5 μm}) in purple, and D_p of 0.5-1.0 μm (particle_{0.5-1.0 μm}) in yellow, and row data in gray open symbol and mean \pm standard deviation of each 500 m altitude range in closed symbol with fence. In (c), the vertical profiles of (b) are shown together in light gray. Altitudes of particular interest are shown by shaded boxes.

Line 356. How would the weather conditions have suppressed condensation of volatiles onto particle surfaces? Please be more specific. The temperature was lower during EOF1, which seems like it would support more rather than less condensation.

Temperature was high during “persistent anticyclone” period (Figure 6).

Line 364-366. The claim in the second sentence is a big claim and it does not follow from the first sentence in this paragraph. It is an interesting claim, and I would encourage the authors to expand upon it. What number fraction of the particles is made up of BC particles? If they were not present, what would happen to the materials that would otherwise condense on them?

This part was rewritten under Sec.3.6.

3.6. rBC as a robust tracer for particle growth in size and mass

In addition to the evolution of nanoparticles, the role of accumulation-mode particles in increasing the aerosol mass was highlighted above. Among aerosol particles, BC is of particular interest, as bare BC particle is insoluble and small, generally peaking below 100 nm in number and thus it potentially provides a chemically inert surface on which volatile substances can condense to form a coating and further grow on. In terms of climate effect, BC has been well established as the second strongest warming agent after CO₂ (Bond et al., 2013). To assess a role of BC particle in aerosol transformation, the mass and mixing state of rBC particles were determined at GCO in Jeju and compared between the two periods of the KORUS-AQ campaign (“persistent anticyclone” and “transport/haze”) (Table 2, Fig. 5f and Fig. 7).

Figure 7a illustrates variations of D_{shell} (optical diameter of rBC-containing particle in a core-shell configuration with rBC core-restricted to 180-220 nm; Sec. 2.1) as a function of PM_{2.5} concentration bin for the entire campaign period. D_{shell} increased almost linearly with PM_{2.5} mass concentration, reaching 300-400 nm on average at PM_{2.5} higher than 40 $\mu\text{g m}^{-3}$. This reveals a close relationship between rBC coating thickness and PM_{2.5} mass enhancements. In Figure 7b, volume concentration of particles_{200-470 nm} was also elevated simultaneously with PM_{2.5} mass concentrations, and rBC coating was obviously thicker (48 ± 39 nm) during “transport/haze” period when the PM_{2.5} mass concentration was highly elevated over the Korean peninsula (Jordan et al., 2020). These results demonstrate that rBC-containing particles with thick coatings are truly representative of accumulation-mode particles in terms of size particularly during “transport/haze” period. Together with the enhanced SIA concentrations and the thicker coating of rBC (Fig. 7b and c), ALWC was as high as 10.3 ± 8.2

$\mu\text{g m}^{-3}$, accounting for 30% of the dry $\text{PM}_{2.5}$ mass (Fig. 7c and Table 2). Given that the RH remained high at greater than 60% during the day and up to 90% at night (Fig. 7b), hygroscopic growth of NH_4NO_3 and $(\text{NH}_4)_2\text{SO}_4$ by uptake of water was expected to be promoted, leading to a large increase in ALWC. SOR was almost linearly increased with RH (Fig. S8b and d). More importantly, sulfuric acid is known to readily condenses on the rBC surface (Kiselev et al., 2010; Zhang et al., 1993, 2008), which provides an active surface for heterogeneous reaction by changing its hygroscopic properties (Khalizov et al., 2009). Hence, the characteristic features observed during the “transport/haze” period suggest an effective condensation of vapors to rBC surfaces and reaction with SIA, resulting subsequent growth of rBC particles in size and mass by forming thick coating on their surfaces (Adachi et al., 2014; Lim et al., 2018; Ueda et al., 2016). The shell size of rBC with a core diameter of 180-220 nm reached approximately 300-400 nm. Given that the $\text{PM}_{2.5}$ concentration increased linearly with the volume concentration of particles_{200-470 nm} (Fig. 7a), the role of internally-mixed BC particles is critical to the increase in mass of fine aerosol, as they provide surfaces for gaseous precursors of SIA to condense on.

In contrast, a thinner coating (29 ± 31 nm) and a lower concentration (by 40%) of rBC particles as well as the low levels of SIA were evident under low RH ($53 \pm 9\%$) conditions during “persistent anticyclone” period. In this case, the organic carbon (OC) fraction was the greatest in $\text{PM}_{2.5}$. ALWC was very low as well, possibly due to less water uptake by the aged organic aerosol (Engelhart et al., 2011). It is likely that the weather condition suppressed the condensation of volatile materials on aerosol surface and thus the secondary aerosol formation on rBC surface. It is also possible that organic materials may form an organic film on the BC surface, inhibiting the vapor uptake for SIA and the increase in rBC coating (Saxena et al., 1995; Sellegri et al., 2003). Instead, they promoted the growth of nucleation- and Aitken-mode particles smaller than 60 nm under low RH conditions (Fig. 7a). The mass size distributions of OC, NO_3^- , and SO_4^{2-} estimated by the aerosol mass spectrometer generally show organics enriched in nucleation-mode particles (e.g., Kang et al., 2018; Kim et al., 2018).

In this regard, rBC particles and their coating thickness are proposed as an agent for generating accumulation-mode particles through SIA formation and as an operational parameter to understand the chemical mechanisms responsible for fine aerosol pollution driven by SIA, respectively. This, in turn, implies that reducing primary emissions of gaseous precursors and BC will be one of the effective ways to combat high $\text{PM}_{2.5}$ mass concentrations in Northeast Asia, especially during the cold months.

Figure 4. Maybe the continent outlines could be in a thicker pen? It's a little hard to make them

out. Please give units for the geopotential height. What timescale do these back trajectories cover? Please state that as well.

Figure 4 was removed in the manuscript and placed in supplementary information (Figure S4).

Figure 7. It's a little difficult to know how to compare the sizes of the circles and squares (i.e. volume vs width). Maybe alongside the scale for the circle size vs. coating thickness you could do the same for the squares in the EOF1 case.

Citation: <https://doi.org/10.5194/acp-2020-1247-RC2>

Figure 7 (& figure caption) was modified and given as Figure 7b and c in the revised manuscript.

Figure 7. Relationships of rBC properties, $PM_{2.5}$ mass and composition, and $particles_{200-470}$ volume concentration measured during the KORUS-AQ campaign. (a) D_{shell} variations as a function of $PM_{2.5}$ concentration for the whole campaign period, (b) relationship between $particles_{200-470}$ volume concentration and $PM_{2.5}$ mass concentration color-coded by rBC mass concentration, and (c) relationship between $PM_{2.5}$ chemical constituents color-coded by RH. In (b) and (c), the marker size is proportional to the rBC coating thickness. D_{shell} and coating thickness are restricted to $180 \text{ nm} \leq D_{rBC} \leq 220 \text{ nm}$.